Feasibility of *in situ* neutron diffraction studies of non-crystalline silicates up to pressures of 25 GPa

2008 J. Phys.: Condens. Matter 20 244122

(http://iopscience.iop.org/0953-8984/20/24/244122)

J. Phys.: Condens. Matter **20** (2008) 244122 (7pp) doi:10.1088/0953-8984/20/24/244122

Feasibility of *in situ* neutron diffraction studies of non-crystalline silicates up to pressures of 25 GPa

Martin Wilding[1], Malcolm Guthrie[2,5], Craig L Bull[2], Matt G Tucker[3] and Paul F McMillan[4]

[1] Institute of Mathematical and Physical Sciences, Aberystwyth University, Aberystwyth, Aberystwyth SY23 3BZ, UK
[2] SUPA School of Physics and Centre for Science at Extreme Conditions, University of Edinburgh, Mayfield Road, Edinburgh EH9 3JZ, UK
[3] ISIS Facility, Rutherford Appleton Laboratory, Chilton, Oxon OX11 0QX, UK
[4] Department of Chemistry and Materials Chemistry Centre, University College London, 20 Gordon Street, London WC1H 0AJ, UK

Received 16 April 2008
Published 29 May 2008
Online at stacks.iop.org/JPhysCM/20/244122

Abstract

There is an increasing interest in the structural modifications found in liquids and amorphous systems as a function of pressure. Neutron diffraction is a key technique for determining these structures, but its application in high pressure studies remains in its infancy. Recent developments now permit *in situ* neutron scattering studies of amorphous materials to very high pressure conditions. Here we present new data for MgO–SiO_2 and SiO_2 glasses collected at up to 8.6 and 24 GPa respectively, using two distinct high pressure anvil geometries. The data collected on the MgO–SiO_2 system appear to be reliable, and suggest strong changes in the chemical ordering. In contrast, the higher pressure SiO_2 data highlight significant difficulties in performing appropriate corrections for pressure-dependent background and attenuation effects. These challenges are discussed, and future improvements to the technique are proposed.

(Some figures in this article are in colour only in the electronic version)

1. Introduction

The thermodynamics of amorphous materials and transport properties in liquids are determined by their atomic scale structure as well as compositional, density or entropy fluctuations involving medium- to long-range correlations. Diffraction measurements of liquids and glasses are powerful probes of this structure, and their implementation under combined high P–T conditions is essential to understanding their physics and chemistry. In particular, neutron diffraction is a key technique, offering both access to information at very high momentum transfers and selectivity of individual correlations via isotope-specific scattering strengths. While significant technical challenges have hitherto limited non-crystalline neutron diffraction at high pressure, recent studies of amorphous ice [1], glassy germania [2] and liquid water [3] have demonstrated the utility of opposed anvil devices of the Paris–Edinburgh type [4–7] for quantitative *in situ* measurements. Here we report initial results from a focused effort to improve both the quality of data analyses and to extend the maximum attainable pressures for this experimental set-up. These techniques will be complimentary to measurements exploiting high-energy synchrotron x-ray scattering with diamond anvil-type [2, 8] or other high pressure cells [9].

We have conducted our investigations using two different samples and two distinct high pressure anvil geometries. Our first sample was MgO–SiO_2 glass, which was studied using anvils with a single-toroidal profile [10], capable of taking $\sim$100 mm^3 volumes up to $\sim$10 GPa [5]. Our second sample was pure SiO_2 glass, for which we used double-toroidal profile anvils to reach pressures approaching 25 GPa with a volume of $\sim$30 mm^3 [5]. Thus, in the latter study, the quality of the diffraction signal is compromised to achieve the highest pressures.

[5] Present address: Advanced Photon Source, Argonne National Laboratory, 9700 S Cass Avenue, Argonne, IL 60439, USA.

Both of these systems had the potential to reveal interesting structural changes at high pressure. It is well known that SiO_2 exhibits an irreversible compaction phenomenon after it has been compressed to 8 GPa [11, 12], that reflects changes in the packing of the tetrahedral network structure. At higher pressures, above ∼20 GPa [12–15], it is known that configurations with increased Si coordination numbers appear, as they do in the crystalline phase, forming the rutile-structured mineral stishovite with octahedrally coordinated SiO_6 groups. Evidence of this transition in the amorphous phase comes from molecular dynamics studies [16], FTIR spectroscopy [14, 15, 17] and amorphous x-ray scattering experiments in a diamond anvil cell using energy-dispersive synchrotron techniques [18]. This work has stimulated suggestions that SiO_2 might undergo a polyamorphic transition between low and high density, strong and fragile forms [19, 20], as a function of pressure [20, 21].

Similarly, high pressure FTIR and Raman spectroscopic studies of the Mg–SiO_2 system in the diamond anvil cell, along with MD simulations, suggest that highly coordinated silicate species begin to appear above ∼20 GPa [15, 17]. Also, at lower pressure, changes in the Mg–O coordination environment may be expected to occur as the relatively open ambient pressure structure [22] compacts to accommodate the increasing density.

In this paper we will discuss the application of neutron diffraction to vitreous silicates using techniques developed at the ISIS facility at the Rutherford Appleton Laboratory, UK. We have exploited existing infrastructure at the HiPr diffractometer—a device already optimized for studying crystalline samples at high pressure—and adapted it for quantitative diffraction measurements of non-crystalline samples. The low backgrounds and high count rates of the HiPr diffractometer yield the possibility of data collection at pressures approaching 25 GPa. Data on both glasses are presented, representing our first steps in investigating the changes in the structure and the structure-related properties (e.g. configurational entropy) of these geologically and technologically important systems. We will discuss the limitations of these data and the potential for future work.

2. Background theory

In a neutron diffraction experiment, an incident beam of thermal neutrons (either mono- or polychromatic) is scattered by a crystalline, liquid or amorphous sample and the intensity of the scattered signal measured as a function of the scattering vector $\boldsymbol{Q}$, which is a function of scattering angle 2θ and neutron wavelength λ_n (or, equivalently, neutron energy E_n). As amorphous structures are isotropic and homogeneous, the only relevant quantity is the *magnitude* of the scattering vector, Q. If we assume that the scattering is elastic, then λ_n is unchanged by its interaction with the sample, and $Q = 4\pi \sin\theta/\lambda_n$. Our measurements use an energy-dispersive, time-of-flight (TOF) technique at the ISIS pulsed spallation neutron source. In a spallation source, a beam of protons is accelerated towards a heavy metal target, where collisions between the incident protons and target nuclei eject high-energy neutrons. These neutrons are then thermalized by multiple collisions with the material of a moderator, which then becomes the effective neutron source for a spectrometer. At ISIS, the incident proton beam is pulsed at a rate of 50 Hz and the generated neutrons exit the moderator with this same period. The TOF technique exploits the fact that the time taken to traverse the distance from moderator to detector is proportional to the neutron wavelength. For non-relativistic neutrons, the relation is given by

$$\lambda_n = \frac{h}{p_n} = \left(\frac{h}{m_n}\right)\frac{T}{L} \tag{1}$$

where h is Planck's constant, p_n and m_n are the neutron momentum and mass, respectively, and L is the total flight path from moderator to detector. Substituting this into the expression for Q above gives

$$Q = \left(\frac{4\pi m_n}{h}\right)\frac{L\sin\theta}{T}. \tag{2}$$

The product $L\sin\theta$ is determined by a calibration measurement using a standard crystalline material of known structure and, thus, Q is known for every incident neutron. The data from all detector elements can be binned in Q and combined to give the differential cross section $\mathrm{d}\sigma/\mathrm{d}\Omega$ as a function of Q. In the absence of energy transfer between neutron and sample nuclei, the differential cross section is entirely elastic and has three parts: self-scattering, which reflects coherently scattered radiation from a single component of the scattering system; distinct scattering, which arises from interference *between* the scatterings from these distinct species, and an *incoherent* scattering component, which is independent of Q and essentially constitutes an unwanted background contribution in a diffraction measurement. The coherent and total scattering cross sections are respectively $\sigma_i^{\mathrm{coh}} = 4\pi\bar{b}_i^2$ and $\sigma_i = 4\pi\overline{b_i^2}$, where the coherent bound scattering length of isotope i, b_i, characterizes the strength of the neutron–nucleus interaction [23]. The quantity b is in general complex and its value depends on the particular isotope and the spin state of the neutron–nucleus system. Thus, scattering lengths can be positive or negative (the latter reflecting 180° phase shift of the scattered neutron) and can vary strongly for different isotopes of a given element.

The differential cross section for a polyatomic system comprises the sum of several partial atom-pair functions and is written as

$$\frac{1}{N}\left[\frac{\mathrm{d}\sigma}{\mathrm{d}\Omega}(Q)\right] = F(Q) + \sum_{\alpha}^{n} c_\alpha \overline{b_{\alpha,\mathrm{inc}}^2} \tag{3}$$

where N is the number of scattering centres and c_α the concentration of chemical species α. $F(Q)$ is the total interference function and gives the distinct scattering. The second term comprises the sum of the self and incoherent scattering components, both of which are independent of Q [24]. It is convenient to express the total interference function $F(Q)$ in terms of a dimensionless static structure factor $S(Q)$ [23], which, in turn, can be

decomposed into partial structure factors using the Faber–Ziman convention [25]:

$$F(Q)\Big/\left(\sum_{\alpha=1}^{n} c_\alpha \overline{b}_\alpha\right)^2 = S(Q) - 1 = \left(\sum_{\alpha=1}^{n} c_\alpha \overline{b}_\alpha\right)^{-2} \times \sum_{\alpha,\beta}^{n} c_\alpha c_\beta \overline{b}_\alpha\ \overline{b}_\beta \left[S_{\alpha,\beta}(Q) - 1\right] \quad (4)$$

Thus, where there are n components, this gives $n(n+1)/2$ partial structure factors, $S_{\alpha\beta}(Q)$, between each pair of species α and β. Other descriptions such as the Bhatia–Thornton formalism have also been used extensively to describe the atom–atom correlation functions in liquid and glassy systems [26].

The sine Fourier transform of $S_{\alpha\beta}(Q)$ leads to the partial pair distribution $g_{\alpha\beta}(r)$ function through

$$g_{\alpha,\beta}(r) - 1 = \frac{1}{2\pi^2 r\rho_0}\int_0^\infty Q\left[S_{\alpha,\beta}(Q) - 1\right]\sin(Qr)\,\mathrm{d}Q. \quad (5)$$

The total number density of atoms is ρ_0, and $g_{\alpha\beta}(r)$ is proportional to the probability of finding an atom β at a distance r from an atom α. A Fourier transform of the total multi-component $F(Q)$ defines the total pair distribution function $G(r)$, which is the weighted sum of all partial pair correlations for neutron diffraction data,

$$G(r) = \frac{1}{2\pi^2 r\rho_0}\int_0^\infty QF(Q)\sin(Qr)\,\mathrm{d}Q = \sum_{\alpha,\beta}^{n} c_\alpha c_\beta \overline{b}_\alpha \overline{b}_\beta \left[g_{\alpha,\beta}(r) - 1\right]. \quad (6)$$

3. Experimental techniques and data analysis

Neutron sources are intrinsically weaker than their synchrotron x-ray counterparts. Correspondingly, experiments must be carried out using relatively large volume apparatuses, which limit the maximum achievable pressures to below that achieved in diamond anvil cell experiments. While novel developments at new neutron facilities (including focusing by super-mirrors) will in the future allow very high pressure experiments with diamond anvil-type cells, currently the highest pressures for diffraction measurements are achieved using toroidal anvils [6]. The Paris–Edinburgh press is one such device, that has been especially developed for neutron scattering studies [5–7, 27]. The HiPr diffractometer at ISIS has been built around and optimized for diffraction measurement using this particular device. In our measurements, samples are compressed between two opposing, toroidal-profile anvils [28] in a Paris–Edinburgh hydraulic press [5]. This arrangement can be used to generate pressures exceeding 10 GPa [5]. Our anvil material was sintered diamond, which offers high neutron transparency and has superior mechanical properties. Under load, these anvils deform a metal gasket of the null scattering TiZr alloy that contains the sample; the resulting decrease in available sample volume leads to an increase in sample pressure. A double-toroidal anvil design was used for the SiO_2 loading, facilitating maximum pressures approaching 25 GPa [6] at the expense of sample volume.

Beads of magnesium silicate glass produced by containerless synthesis [29] were crushed to a fine powder and pressed into a pellet that fitted into the single-toroid anvil. For SiO_2, in order to limit the reduction of volume as a powder is compressed, a commercially available vitreous SiO_2 rod was cut and machined to make a solid pellet that fitted into the double-toroid sample space.

In the configuration used at HiPr, a well collimated beam of incident neutrons is directed down the compression axis of the cell—through one of the anvils—to reach the sample. The diffracted neutrons exit through the TiZr gasket and outer parts of the anvil, and are detected by 15° wide detector banks centred on 90°. The resulting access to reciprocal space is limited to 1.5–20 Å^{-1}. Diffraction experiments on amorphous/glassy systems are inherently more challenging than equivalent measurements on crystalline systems. This is particularly true at high pressure, as a consequence of a small sample volume, limited diffraction aperture and often bulky sample environment. Consequently, even at high flux sources, such as ISIS, long counting periods (up to 24 h) were required to determine the diffraction pattern with sufficient statistical accuracy for analysis. Additional background measurements were also necessary, taking the same time as the sample data collection.

A central challenge in extracting the structure factor, $S(Q)$, is that the background arising from the pressure cell (and predominantly due to anvil scattering) is, itself, pressure dependent. This background can be decomposed into sharp Bragg features and a broad diffuse background. Additionally, superimposed on this are pronounced 'Bragg edges' resulting from enhanced transmission of neutrons through polycrystalline material (the diamond anvils themselves) that are above the limiting wavelength for which Bragg diffraction can occur for a given set of lattice planes [30].

In correcting our data, an experimental background was measured for each pressure point. In these measurements, the sample was removed, the cell re-assembled and a hydraulic load of 5 tons applied to stabilize the assembly. This approximate background was found to differ from the *in situ* background in three ways. (1) It was necessary to apply a constant scale factor to account for elastic expansion of the gasket and the consequent increase in the diffraction aperture in the background measurement. This was readily estimated by measuring the intensity of diamond Bragg peaks in both *in situ* and background measurements. (2) The diamond Bragg peaks were broadened and shifted in the *in situ* measurement as a result of anvil strain. To correct this, the diamond Bragg peaks in both background and sample measurements were fitted using a Lebail technique [31] and subtracted. (3) There was a subtle shifting of broad features in the background that we believe are related to multiple scattering within the anvils. At lower pressures this appears to contribute only weakly to the resulting $S(Q)$ data; however, at the highest pressures achieved in our SiO_2 loading this is an important source of error as discussed below.

In addition to background subtraction, it is necessary to apply a correction for both anvil and gasket attenuation of the neutron beam (here we have explicitly ignored the sample

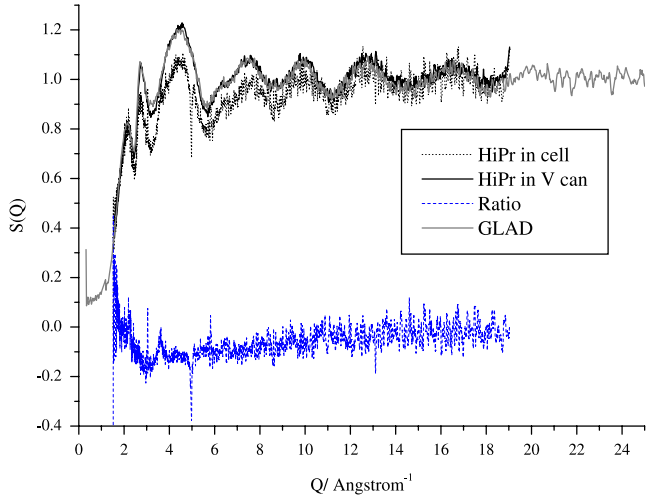

Figure 1. The $S(Q)$ data for 62% MgO–38% SiO_2 glass determined at GLAD (IPNS) and at HiPR (ISIS) both in vanadium canisters at ambient pressure. There are no significant differences between the two data sets, indicating that inelastic contributions are minimal. Also shown is the $S(Q)$ for the same glass as measured in the pressure cell, which exhibits more pronounced differences, attributed to errors in the attenuation correction procedure. The blue curve shows the ratio between the in- and out-of-cell data, which provides a multiplicative 'modification' function that can be applied to the data. Sharp features visible at 3 and 5 Å^{-1} in the pressure cell data arise from residual anvil Bragg intensities.

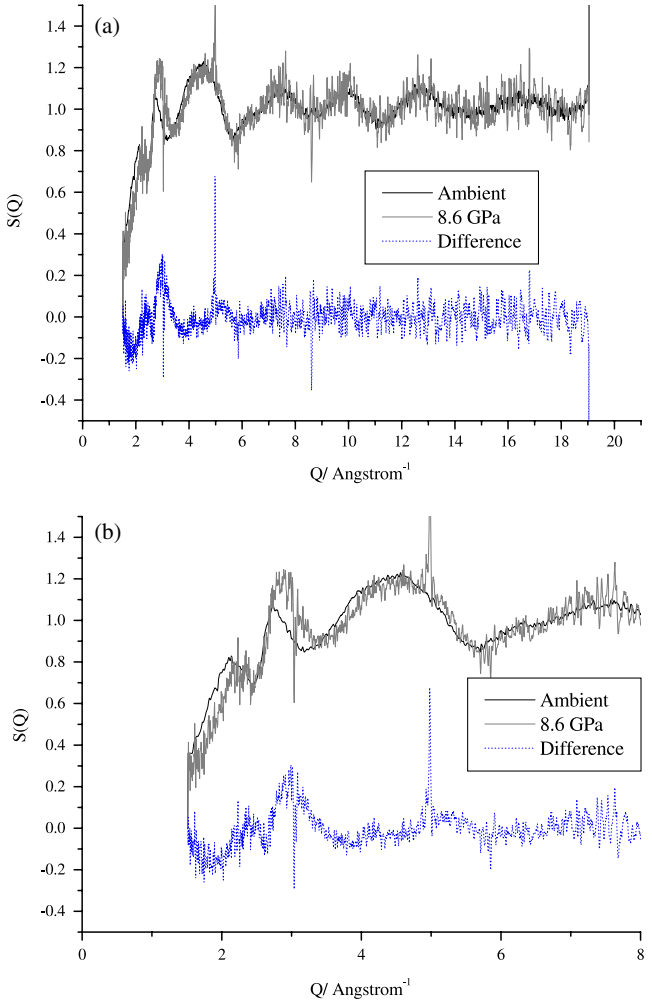

Figure 2. (a) $S(Q)$ data for 62% MgO–38% SiO_2 glass measured up to 8.6 GPa at HiPr. There are clear changes in the $S(Q)$ as the sample is compressed that are highlighted by the difference curve at the base of the figure. These comprise shifts in the first peak from 2.0 to 2.3 Å^{-1} and a shift in the position of the peak at 2.75 Å^{-1}. There are other changes at higher Q seen as an increase in the signal in the 3 Å^{-1} range, and also there is a shoulder to the peak at 4.5 Å^{-1}. (b) The same data plotted in the low-Q region. The residual diamond peaks are more pronounced in the high pressure data set; however, they remain small enough to not affect the data strongly.

self-attenuation, which is negligible for our small sample sizes). Our initial approach was to use the semi-empirical correction that is applied as standard for correcting crystalline diffraction patterns on HiPr. This is generated by measuring the neutron transmission per unit length of each component of the assembly (at ambient pressure), and then calculating the integrated attenuation along the composite path lengths through the pressure cell to the detector. However, we found that the resulting $S(Q)$ data were not adequately corrected, as shown by the comparison with the 'out of cell' data, measured in a vanadium canister on HiPr (see figure 1). In contrast with crystalline data, where the only important intensities are those of Bragg peaks, an amorphous pattern constitutes a far more stringent test of the attenuation procedures. In order to correct the calculated attenuation function, we took the ratio of the resulting $S(Q)$ with one in a vanadium can. This provides a 'modification' function that corrects the error in the calculated attenuation (this function is also shown in figure 1). As with the background correction, there is no guarantee that the attenuation is not pressure dependent; however, minimal distortion of the diamond microstructure (probed by the crystalline diffraction of the anvil material) indicates that this effect is not too severe for the lower pressure MgO–SiO_2 data set. Correspondingly, we believe that the 8.6 GPa $S(Q)$ for the magnesium silicate sample, which was corrected using the ambient pressure modification function (shown in figure 3), remains quantitatively correct.

In the final stage of analysis, background subtracted and attenuation corrected diffraction data are multiplied by a constant scale factor to ensure that they oscillate about the self-scattering of the sample scattering unit at high Q. This scaling takes no account of any inelastic component of the scattering. The lightest nuclei in the sample are those of oxygen, and these are sufficiently heavy that a standard Plazcek correction applies. This correction is known to have a pronounced dependence on scattering angle. Therefore, the similarity of the MgO–SiO_2 $S(Q)$ data measured on HiPr at 90° and the equivalent dataset from GLAD [22] measured at low angles demonstrates that the effect is negligible. In interpreting our high pressure data, we have made the reasonable assumption that the magnitude and nature of this effect remains small at higher pressures.

A further challenge in these measurements is accurate determination of the sample pressure. As the anvil material is optically opaque, standard ruby fluorescence determination of pressure is not possible. Additionally, and in contrast

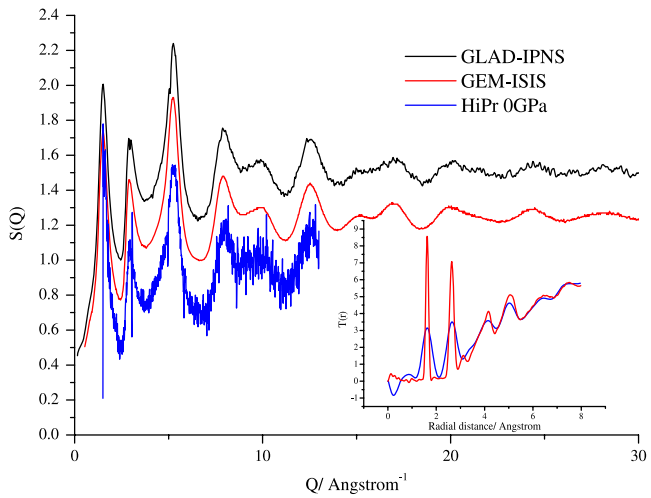

Figure 3. $S(Q)$ data at ambient pressure for vitreous SiO_2 obtained at GLAD (IPNS), GEM (ISIS) and inside the pressure cell at HiPr (ISIS). The restricted Q range of the HiPr configuration and decreased signal quality are evident. The inset shows total radial distribution functions in the form $T(r) = 4\pi\rho r G(r)$ (where ρ is the sample density) taken from both the GEM and in-cell HiPr data. It is clear that, despite the limitations of the data, the main structural features of the silica structure are retained. The greater maximum Q value and corresponding real-space resolution of the GEM data is highlighted by the sharp peak widths in the transform. However, we note that the high *minimum*Q value obtainable on PEARL (that results in a truncated FSDP) has no pronounced effect on the radial distribution functions.

to a crystalline sample, the density of glassy or amorphous matter cannot be easily extracted from the diffraction pattern itself. In this study, a calibration measurement was performed where a mixture of crystalline MgO powder was combined with the sample glass. By using MgO, we tried to ensure that the compressibility of the sample and calibrant were approximately the same. The known equation of state of MgO was then used to convert the refined unit cell volume, at a given hydraulic load, to a sample pressure. The resulting pressure–load curve was then assumed to be the same for subsequent loadings of pure glass. However, subtle differences in quality of the loadings can have a pronounced effect on the actual pressure; therefore, the quoted pressures are subject to an estimated experimental uncertainty of ± 0.5 GPa. Broadening of the crystalline MgO peaks in the calibration sample indicated the presence of non-hydrostaticity in the sample. This is to be expected for a relatively hard sample material under uniaxial compression, and is unavoidable; the diffraction signal from a—typically liquid—hydrostatic medium would be impossible to subtract from that of the sample.

4. *In situ* neutron diffraction from magnesium silicate glass at high pressure

Diffraction data for the magnesium silicate glass were measured for a total of 24 h. To determine the background, the cell was re-assembled using the recovered, deformed TiZr gasket, and a hydraulic load of 5 tons applied to stabilize the assembly. The background measurement was also collected for 24 h to ensure equivalent counting statistics.

The measured diffraction patterns were converted into $S(Q)$ using the procedures described in the preceding section. In figure 2 we contrast the $S(Q)$ data for the 38% SiO_2 magnesium silicate glass at ambient pressure and *in situ* at 8.6 GPa. The difference between these two data sets is also shown (figure 2(a)). At high Q, the 8.6 GPa data are identical within the experimental noise to the ambient pressure data. This implies that that there is little or no change in the short range order (or first neighbour coordination shell) that gives rise to the fundamental oscillation in the $S(Q)$. Further, it can be shown, by using the approach of Narten [32], that Mg–O and Si–O short range correlations dominate the peak at 4.5 Å^{-1} in the $S(Q)$. This peak exhibits only minor changes as pressure is applied, and it is reasonable to assume that our data show that no increase in Si–O coordination number is observed up to 8.6 GPa. This is not surprising as, in pure SiO_2, $^{[VI]}$Si is not formed below pressures of 28 GPa [18], much higher than the 8.6 GPa of this experiment.

There are, however, pronounced changes in the first two peaks of $S(Q)$, with both shifting to higher Q with increasing pressure (figure 2(b)). The first peak in the diffraction pattern at 2.0 Å^{-1} shifts to 2.2 Å^{-1} and appears to lose intensity by 8.6 GPa. This is a chemical ordering peak and the pressure-induced changes reflect changes in the connectivity of Mg–O and Si–O coordination polyhedra. The peak at 2.7 Å^{-1} also shifts to higher Q (2.85 Å^{-1}), but gains intensity. We cannot assign directly the corresponding changes in real space, but we can speculate that the increase in Q of the first peak is related to a shortening length scale in the chemical ordering in response to pressure. Distortion and densification of the intermediate range structure has been shown to be a precursor of local coordination change in GeO_2 [2]; it is possible that a similar mechanism occurs in magnesium silicate.

5. *In situ* neutron diffraction from vitreous SiO_2 at high pressure

A double toroid anvil configuration was used for the study of vitreous silica, allowing higher pressures to be achieved [6]. However, the sample volume is smaller and, as pressure is applied, the gap between anvils becomes extremely small, limiting the aperture for the diffracted beam. The anvil separation for a given pressure can be maximized by ensuring 100% packing fraction of the sample. This was achieved by using solid pellets of vitreous SiO_2 ground from a glass rod to match the sample chamber geometry. Despite this, it was still necessary increase the gap in Cd shielding that is normally used to absorb anvil scatter in order to maintain signal levels, with the unfortunate consequence that the background from the diamond anvils (both Bragg and diffuse) is significantly strengthened. The resulting poor subtraction of the anvil Bragg peaks is clearly evident in the $S(Q)$ data shown in figure 4. In addition, the pressure dependence of the diffuse background and of the Bragg edge structure in the attenuation becomes worse in the higher pressure

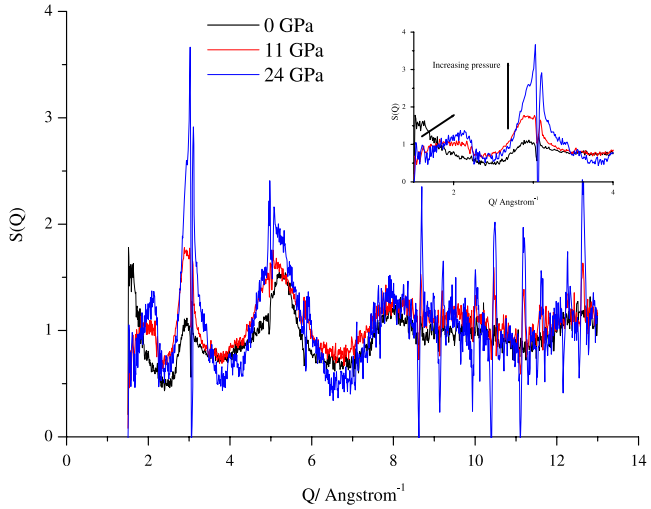

Figure 4. A summary of the changes observed in the diffraction pattern of vitreous SiO_2 with increasing pressure. Data have been corrected using the same procedures as employed for the MgO–SiO_2 glasses, although the failure of these at the highest pressures is the likely cause of strong enhancement of the peak at $\sim$3 Å^{-1} and the new feature visible at 4 Å^{-1}. The inset highlights the shift of the first sharp diffraction peak to higher Q. As peak positions are less strongly affected by error in the corrections employed, it is likely that this motion is a real effect. The sharp features represent incomplete removal of diamond Bragg peaks from the pressure cell, which are significantly worse than in the MgO–SiO_2 data sets.

study; the ambient pressure characterization of these artefacts becomes increasingly inaccurate as the anvil microstructure itself changes. However, despite these limitations, it is encouraging that a reasonable signal level from the sample is retained up to our highest pressure.

In figure 3 we show the $S(Q)$ for SiO_2 at ambient pressure enclosed in the pressure cell. This is compared with SiO_2 data from IPNS (GLAD) and ISIS (GEM) that show the richness of structure of this important amorphous material. The configuration at HiPr means that the lowest Q available is 1.5 Å^{-1}, truncating the first peak in the SiO_2 $S(Q)$, known as the first sharp diffraction peak (FSDP). Even with counting times of 48 h, the diffraction data are noisy, and above $\sim$13 Å^{-1} are dominated by anvil Bragg scattering. The resulting truncated Q range limits the accuracy of the normalization, and gives a poor resolution in the real-space transform. In comparison, ambient pressure $S(Q)$ data for amorphous samples can routinely be obtained to values of Q in excess of 50 Å^{-1} [33]. Even though there is a limited Q range, the main features of the $S(Q)$ for vitreous SiO_2 are reproduced; the difference between the HiPr and GEM data is shown and this too indicates a failure of the attenuation correction. As with the MgO–SiO_2 data, it is possible to obtain a modification function that is applicable at lower pressure. However, strong changes in the anvil microstructure at the highest pressures mean that, in contrast to the single-toroid case, this simplistic approach is no longer sufficient to accurately correct the data.

The high pressure SiO_2 data are corrected using a similar approach to that adopted for the single-toroidal anvil configuration. An experimental background was measured for both 11 and 24 GPa pressure points using the recovered, deformed TiZr gasket as with the MgO–SiO_2 measurements. Unfortunately, the dependences of both this background and the attenuation correction on pressure render any quantitative conclusions impossible. While the intensities of the peaks are almost certainly unreliable, the shift to higher Q of the FSDP by 11 GPa can be believed with some confidence. Moreover, it is interesting that this shift appears to be far smaller from 11 to 24 GPa. This suggests that the collapse of the intermediate range structure probed by the FSDP mostly is complete by 11 GPa. The substantial increase in the intensity of the second peak with pressure is most likely attributable to background scaling issues, although the apparent increase in the width of this peak may be a real feature of the structure.

6. Future directions

Neutrons offer the opportunity to determine the structure of amorphous materials at pressures of up to 24 GPa. We have demonstrated that up to $\sim$9 GPa large volumes and low anvil strains facilitate quantitative neutron $S(Q)$ determination. At higher pressures, while a reasonable signal level is retained, an enhanced background and the difficulty of determining *in situ* attenuation and background corrections strongly limits the utility of the measured data. High quality diffraction data at these pressures will require significant improvements to the experimental methodology.

To this end, we have already begun to investigate modified collimation and shielding that will further minimize background scattering and, in particular, reduce the structure in the background arising from coherent anvil scattering. Initial tests have indicated that measurements of pressurized vanadium pellets in place of the sample can be used to extract the pressure dependence of the Bragg edge effects in the attenuation of the sintered diamond anvils. An additional promising direction is the use of *in situ* transmission measurements coupled with Bragg edge refinement software to obtain accurate attenuation determinations at high pressure.

We have demonstrated that neutron diffraction information from glassy silicates is, in principle, achievable up to pressures approaching 25 GPa. And we have clarified some of the main analysis problems that must be addressed to make these data quantitative. An additional context to this work is provided by the imminent arrival of new neutron sources and instruments [34] such as SNAP at the Spallation Neutron Source, Oak Ridge National Laboratory (USA). In addition, developments continue at HiPr, and new instruments will soon become available at a second target station at ISIS. It is likely that over the next decade diffraction measurements from amorphous and liquid samples at high pressure will become increasingly accurate and routine.

Acknowledgments

We would like to thank STFC for access to the ISIS Facility at the Rutherford Appleton Laboratory. We also acknowledge the technical support of D J Francis during the experiments.

Technique developments for this work were supported through EPSRC funding. We would like to acknowledge the assistance of Chris Benmore and Joan Siewenie at the Intense Pulsed Neutron Source (IPNS) in preliminary experiments that were performed at GLAD; sadly, this facility is now closed. This study has been in part supported by the Aberystwyth University Research fund and the Higher Education Funding Council for Wales through the Centre for Advanced Functional Materials and Devices (CAFMaD) and also by COMPRES, the Consortium for Materials Properties Research in Earth Sciences under the NSF (US) cooperative agreement EAR 01-35554. Contributions of PFM were supported by the EPSRC via portfolio grant EP/D504872 and senior research fellowship EP/D07357X. Support for travel to the European Science Foundation meeting in Ustron was provided by the Gooding Fund, Aberystwyth University.

References

[1] Klotz S *et al* 2002 *Phys. Rev. Lett.* **89** 0285502
Klotz S *et al* 2005 *Phys. Rev. Lett.* **94** 285506
Nelmes R J *et al* 2006 *Nat. Phys.* **2** 414
[2] Guthrie M *et al* 2004 *Phys. Rev. Lett.* **93** 115502
[3] Strassle T *et al* 2006 *Phys. Rev. Lett.* **96** 067801
[4] Besson J M *et al* 1995 *High Pressure Res.* **14** 1
Loveday J S *et al* 1996 *High Pressure Res.* **14** 303
[5] Besson J M *et al* 1992 *Physica* B **180** 907
[6] Klotz S *et al* 1995 *Appl. Phys. Lett.* **66** 1735
[7] Le Godec Y *et al* 2004 *High Pressure Res.* **24** 205
[8] Mei Q *et al* 2007 *J. Non-Cryst. Solids* **353** 1755
[9] Le Godec Y 2005 *High Pressure Res.* **25** 243
[10] Khvostantsev L G 2004 *High Pressure Res.* **24** 371
[11] Hemley R J *et al* 1986 *Phys. Rev. Lett.* **57** 747
Hemley R J, Prewitt C T and Kingma K J 1994 High-pressure behavior of silica *Silica: Physical Behavior, Geochemistry And Materials Applications* vol 29 (Washington, DC: Mineralogical Society America) p 41
Susman S *et al* 1991 *Phys. Rev.* B **43** 11076
[12] Wolf G H and McMillan P F 1995 *Structure, Dynamics and Properties of Silicate Melts* vol 32 (Washington, DC: Mineralogical Society America) p 505
[13] Williams Q *et al* 1993 *J. Geophys. Res.* B **98** 22157
[14] Williams Q and Jeanloz R 1988 *Chem. Geol.* **70** 91
[15] Williams Q and Jeanloz R 1988 *Science* **239** 902
[16] Kubicki J D and Lasaga A C 1988 *Am. Mineral.* **73** 941
Woodcock L V, Angell C A and Cheeseman P 1976 *J. Chem. Phys.* **65** 1565
[17] Williams Q, Jeanloz R and McMillan P 1987 *J. Geophys. Res.* B **92** 8116
[18] Meade C, Hemley R J and Mao H K 1992 *Phys. Rev. Lett.* **69** 1387
[19] Poole P H and Angell C A 1996 *Abstr. Pap. Am. Chem. Soc.* **212** 211
[20] Poole P H, Saika-Voivod I and Sciortino F 2005 *J. Phys.: Condens. Matter* **17** L431
Saika-Voivod I, Poole P H and Sciortino F 2001 *Nature* **412** 514
Saika-Voivod I *et al* 2004 *Phys. Rev.* E **70** 061507
Saika-Voivod I *et al* 2005 *Phil. Trans. R. Soc.* A **363** 525
[21] Poole P H *et al* 1995 *Comput. Mater. Sci.* **4** 373
Saika-Voivod I, Sciortino F and Poole P H 2004 *Phil. Mag.* **84** 1437
[22] Wilding M C *et al* 2004 *Europhys. Lett.* **67** 212
[23] Keen D A 2001 *J. Appl. Crystallogr.* **34** 172
[24] Fischer H E, Barnes A C and Salmon P S 2006 *Rep. Prog. Phys.* **69** 233
Fischer H E, Salmon P S and Barnes A C 2003 *J. Physique* **103** 359
[25] Faber T E and Ziman J M 1965 *Phil. Mag.* **11** 153
[26] Salmon P S *et al* 2005 *Nature* **435** 75
Salmon P S and Petri I 2003 *J. Phys.: Condens. Matter* **15** S1509
[27] Klotz S, Besson J M and Hamel G 2006 *High Pressure Res.* **26** 277
[28] Khvostantsev L G, Slesarev V N and Brazhkin V V 2004 *High Pressure Res.* **24** 371
[29] Tangeman J A *et al* 2001 *Geophys. Res. Lett.* **28** 2517
Weber J K R *et al* 1994 *Rev. Sci. Instrum.* **65** 456
[30] Fermi E, Sturm W J and Sachs R G 1947 *Phys. Rev.* **71** 589
[31] Lebail A, Duroy H and Fourquet J L 1988 *Mater. Res. Bull.* **23** 447
[32] Narten A H 1972 *J. Chem. Phys.* **56** 1905
[33] Hannon A C 2005 *Nucl. Instrum. Methods Phys. Res.* A **551** 88
[34] McIntyre G J *et al* 2005 *J. Phys.: Condens. Matter* **17** S3017
Parise J B 2006 *Neutron Scatter. Earth Sci.* **63** 205